# Critical Role of Chromium (Cr)−DNA Interactions in the Formation of Cr-Induced Polymerase Arresting Lesions†

Travis O'Brien, H. George Mandel, Daryl E. Pritchard, and Steven R. Patierno*

*Department of Pharmacology, The George Washington University Medical Center, 2300 I Street NW, Washington, D.C. 20037*

*Received July 3, 2002; Revised Manuscript Received August 14, 2002*

ABSTRACT: The genotoxicity associated with the metabolic reduction of hexavalent chromium [Cr(VI)] is complex and can impede DNA polymerase-mediated replication in vitro. The exact biochemical nature of Cr-induced polymerase arresting lesions (PALs) is not understood, but is believed to involve the formation of Cr−DNA interstrand cross-links (ICLs). The aim of this investigation was to determine the dependence of direct Cr−DNA interactions on the development of PALs in DNA treated with trivalent Cr [Cr(III)] or with Cr(VI) in the presence of ascorbic acid (Asc), a major intracellular reductant, using an in vitro, acellular system. The formation of Cr−DNA adducts, ICLs, and PALs was maximal at Asc:Cr(VI) molar ratios of 0.5−2, but gradually decreased at higher ratios. EDTA, a Cr(III) chelator, significantly decreased Cr−DNA binding and ICL and PAL formation. Co-treatment of DNA with Cr(VI)/Asc and mannitol, a Cr(V) chelator, selectively inhibited the formation of mono/bifunctional DNA adducts and PALs produced by Cr(VI) reduction, but had no effect on Cr(III)−DNA binding or Cr(III)-induced polymerase arrest. Blocking Cr−DNA phosphate interaction by preincubation of DNA with $MgCl_2$ abrogated DNA binding and ICL and PAL production. DNA strand breaks and abasic sites may lead to the in vitro arrest of DNA polymerases; however, we failed to detect significant increases in the frequency of these lesions following Cr(VI)/Asc treatment. These data indicate that the bifunctional adduction of Cr to DNA phosphates (ICLs) constitutes a major PAL. Furthermore, the generation of DNA strand breaks and abasic sites by Cr(VI) reduction is insufficient to explain PALs observed in vitro.

The carcinogenic potential of chromium-containing compounds has been intensively investigated and recently reviewed (*1*−*3*). Chromium, in its hexavalent state [Cr(VI)], is relatively inert. Under physiological conditions, Cr(VI), as a chromate oxyanion, enters the cell through nonspecific anionic transporters (*3*−*5*). Within the cell, Cr(VI) is metabolically reduced by ascorbic acid (Asc), glutathione (GSH), or cysteine (Cys) to Cr(III), the most stable form of Cr. Cr(III) is unable to pass easily through the cell membrane and, therefore, remains within the cell bound to macromolecules, where it can attain millimolar concentrations (*6*). During the reduction of Cr(VI), several reactive Cr species, including Cr(IV) and Cr(V), are generated (*7, 8*). While Cr(VI) does not interact with nucleic acids, Cr(III) and Cr(V) display reactivity toward DNA (*8, 9*). In addition to the formation of reactive Cr species, carbon-based and oxygen radicals can be generated during Cr reduction (*7, 8, 10*).

The genotoxicity of chromium is complex and is characterized by damage to DNA bases and the sugar−phosphate backbone. Specifically, the metabolic reduction of Cr(VI) can lead to the formation of Cr−DNA base and/or phosphate monoadducts, DNA strand breaks, oxidatively damaged bases, protein−Cr−DNA cross-links (Cr−DPC), abasic sites, and DNA−Cr−DNA interstrand cross-links (ICLs) (*11*−*16*). Various studies have reported the reduced processivity and guanine-specific arrest of DNA polymerases using Cr-reacted DNA as a template (*12, 17*−*20*). Several Cr-induced DNA lesions (abasic sites, DNA strand breaks, ICLs, oxidized bases) (*15, 21, 22*) could possibly account for the observed in vitro arrest of DNA polymerase on Cr-treated DNA; however, Cr monoadducts and Cr−DPC (GSH) do not constitute polymerase arresting lesions (PALs) (*20*). The guanine-specific attenuation of DNA and RNA polymerase activity on Cr-treated DNA has been associated with ICLs (*12, 18, 23*). Cr-induced ICLs are believed to involve the bifunctional adduction of Cr to (i) phosphate residues in complementary strands of DNA (phosphate−Cr−phosphate cross-links) and/or (ii) guanine residues (guanine−Cr−guanine cross-links) in DNA (*2, 12, 18*). Nevertheless, conclusive experimental evidence linking either lesion to PAL development is not yet available.

The formation of DNA damage by Cr may proceed through direct (Cr−DNA interactions) and/or indirect (oxygen/carbon radicals) mechanisms, but the relative role that each pathway plays in Cr-induced polymerase arrest is not known. To elucidate the relative contributions of these mechanisms to the formation of PALs, we have examined the formation of these lesions under different biochemical conditions in DNA treated with Cr(VI) in the presence of the major intracellular reductant of chromium, Asc, and with Cr(III). Our results suggest that the development of PALs is highly dependent upon direct Cr−DNA interactions involving the bifunctional adduction of Cr to the DNA phosphate back-

† This work was supported by NIH Grant ES05304 to S.R.P.

* To whom correspondence should be addressed at the Department of Pharmacology, The George Washington University Medical Center, 2300 I Street NW, Washington, DC 20037. Tel: (202) 994-3286, Fax: (202) 994-2870, Email: phmsrp@gwumc.edu.

10.1021/bi020452j CCC: $22.00 
Published on Web 09/13/2002

bone. Although DNA strand breaks and AP sites may lead to the in vitro arrest of DNA polymerases, these lesions were undetectable under conditions where adducts, ICLs, and PALs were easily detected and modulated. Thus, their potential contribution to Cr-induced polymerase arrest is minor relative to the contribution of ICLs.

## MATERIALS AND METHODS

*Cell Culture and Reagents.* Human lung fibroblasts (HLF) (ATCC LL-24 cells, 151-CCL) were grown in F12K medium (Life Technologies, Gaithersburg, MD) containing 15% fetal bovine serum (FBS) and supplemented with 0.5% penicillin−streptomycin in a humidified incubator under 5% $CO_2$ at 37 °C. Sodium chromate [$Na_2CrO_4$, Cr(VI)] (J. T. Baker Chemical, Phillipsburg, NJ), ascorbic acid (Fisher Scientific, Fair Lawn, NJ), and mannitol and chromium chloride [$CrCl_3$, Cr(III)] (Sigma Chemical Co., St. Louis, MO) were prepared fresh in sterile water prior to each experiment. Magnesium chloride ($MgCl_2$) (Sigma Chemical Co.), *N*-(2-hydroxyethyl)-piperazine-*N*′-2-ethanesulfonic acid (HEPES), and EDTA (ethylenediaminetetraacetic acid) (Fisher Scientific) were maintained as stock solutions. The construction of the pSV2neoTS vector was reported previously (*18*). All plasmid purifications were performed using the QIAGEN Plasmid Maxi Kit (QIAGEN, Inc., Valencia, CA).

*Preparation and Treatment of Human Lung Fibroblast Genomic DNA.* HLF cells were harvested, and DNA was isolated using the Wizard Genomic DNA Purification Kit (Promega Corp., Madison, WI) as per the manufacturer's protocol. After digestion with *Eco*RI, HLF DNA (0.04 $\mu$g/$\mu$L) was incubated at 37 °C for 2 h in the presence either of Cr(VI) plus Asc or of Cr(III), with and without the addition of other reagents. In all experiments no effects were observed in reactions containing Cr(VI) or Asc alone. Although the concentrations of Cr used in this study are highly toxic to cultured cells, these doses are relevant in cell-free systems due to the significant intracellular accumulation of Cr to millimolar levels (*6*).

*Measurement of Cr(VI) Reduction.* Cr(VI) reduction by ascorbate was monitored by absorption spectroscopy (*24*). Absorbance at a wavelength of 372 nm [$OD_{372}$, the $\lambda_{max}$ of Cr(VI)] reflects Cr(VI) concentration in a linear dose-dependent manner but does not correlate with the other forms of Cr such as Cr(V), Cr(IV), or Cr(III) (*24*). Reactions were carried out under the same conditions as employed for the DNA binding and polymerase arrest assays, but in the absence of DNA. Briefly, Cr(VI) was incubated with ascorbate in 100 mM HEPES, pH 7.4, for 2 h at 37 °C (1 mL final volume). $OD_{372}$ was measured, and the data were expressed as the percent of Cr(VI) remaining.

*Measurement of Total Cr−DNA Binding.* Chromium stock solutions were prepared prior to each experiment by mixing unlabeled Cr(VI) or Cr(III) with radioactive $Na_2{}^{51}CrO_4$ (612 mCi/mg of Cr) or $^{51}CrCl_3$ (564 mCi/mg of Cr, both from ICN, Irvine, CA), respectively. Solutions containing $^{51}$Cr-labeled Cr(VI) or Cr(III) were incubated with 1 $\mu$g of HLF DNA (0.04 $\mu$g/$\mu$L) in 100 mM HEPES (pH 7.2), in the presence or absence of other compounds, for 2 h at 37 °C in a final volume of 25 $\mu$L. Following treatment, 500 $\mu$L of ice-cold 5% trichloroacetic acid (TCA) was added to each reaction which was then incubated for 30 min on ice to allow for precipitation. Samples were placed onto a 5% TCA pre-wetted Whatman GF/A glass micro fiber filter in a vacuum filtration apparatus (Hoefer Scientific Instruments, San Francisco, CA). Filters were washed twice with 5 mL of 5% TCA and twice with 1 mL of methanol and then dried. The amount of $^{51}$Cr remaining on the filter was counted in 5 mL of EcoLite scintillation cocktail (ICN, Irvine, CA). After correction for nonspecific filter binding, Cr−DNA adducts were calculated and expressed as total Cr adducts/1.5 kb (pmol of Cr/pmol of DNA bases) based on the $^{51}$Cr-labeled Cr(VI) or Cr(III) stock solutions.

*Quantitative PCR Analysis of Cr-Treated Human DNA.* Following treatment, genomic DNA was filter-dialyzed against sterile, deionized water using Microcon filter columns (10 000 MWCO) (Millipore, Bedford, MA) to remove unreacted Cr, Asc, and other compounds. DNA concentration was determined by absorption spectroscopy ($A_{260}$). The p53 gene (exons 5−8, ∼1.5 kb) was used as the target sequence for quantitative PCR analysis (QPCR) from chromium-treated HLF DNA using previously published primers (*20*). All reactions were carried out for 28 cycles of amplification using 100 ng of template DNA and 2 $\mu$Ci of [$\alpha$-$^{32}$P]dCTP (3000 Ci/mmol) (ICN, Costa Mesa, CA). Under these conditions, the amount of detectable PCR product was linearly related to template concentration. PCR reactions were admixed with 6× loading buffer and resolved on a 5% nondenaturing acrylamide gel at 200 V, or on a 1% vertical agarose gel at 85 V, for 2 h in 1× Tris−borate−EDTA (TBE), pH 8.3. Gels were dried under vacuum and exposed to film for 3−24 h at −70 °C. Assuming a random distribution of Cr-induced polymerase arresting lesions, the lesion frequency per 1.5 kb was determined from the densitometric data by the Poisson distribution:

$$\mathrm{LF_{PAL}} = -\ln\left(\mathrm{amplification_{Cr\ treated}}/\mathrm{amplification_{untreated}}\right)$$

*DNA Interstrand Cross-Link Detection in Plasmid DNA.* The existence of DNA interstrand cross-links in *Eco*RI-linearized pSV2neoTS DNA was detected using Renaturing Agarose Gel Electrophoresis (RAGE) as previously described (*12*, *18*). Briefly, DNA was reacted with Cr(VI) and various concentrations of Asc for 2 h at 37 °C, filter-dialyzed against sterile, deionized water, and quantified. An aliquot of each sample (50−100 ng) was heat-denatured at 95 °C for 10 min and flash-cooled in an ice bath to prevent reannealing. The denatured samples, along with a nondenatured aliquot of each reaction, were resolved on a 0.8% agarose gel at 35 V overnight. DNA was blotted overnight onto a nitrocellulose membrane by alkaline capillary transfer. Membranes were hybridized to a random hexamer-labeled (Prime-It RmT, Stratagene, La Jolla, CA) 0.95 kb fragment (obtained from a *Pst*I digest of pSV2neoTS) and exposed to film at −70 °C for 3 h or overnight. ICLs were calculated densitometrically as the percent of total DNA existing as dsDNA after heat-denaturation.

*Plasmid Relaxation Assay.* pSV2neoTS DNA (0.04 $\mu$g/$\mu$L) was incubated with 0−120 $\mu$M Cr(VI) and Asc at the indicated molar ratios with or without the addition of EDTA, mannitol, or $MgCl_2$ for 2 h at 37 °C, as described under Results. Following treatment, samples were admixed with 6× gel loading buffer, and aliquots (0.2−0.4 $\mu$g) were resolved on a 1% 1× TBE agarose gel. Gels were stained

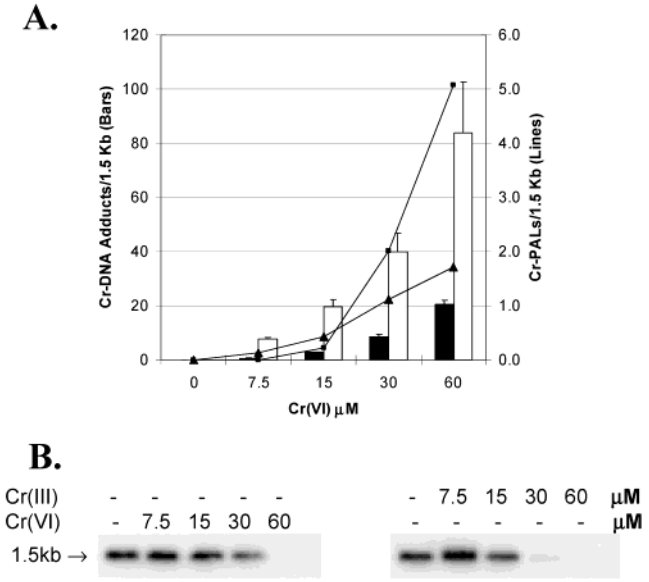


FIGURE 1: Concentration-dependent formation of Cr−DNA adducts and PALs by Cr(VI)/Asc [Asc:Cr(VI) ratio of 0.5] or Cr(III) following a 2 h treatment. (A) $^{51}$Cr−DNA binding (bars) to HLF DNA (0.04 $\mu$g/$\mu$L) treated with increasing Cr(VI) concentrations (closed bars) or Cr(III) (open bars). PAL formation [Cr(VI), triangles; Cr(III), squares] in HLF DNA was quantified by QPCR. (B) Representative gel showing PAL analysis of p53 target sequence (1.5 kb) in Cr(VI)/Asc (left gel) or Cr(III) (right gel) treated HLF DNA. The data are the mean and standard error from at least three independent experiments.

with ethidium bromide and visualized using an Eagle Eye gel documentation system (Stratagene, La Jolla, CA).

*Measurement of Abasic Sites in Plasmid DNA.* pBR322 DNA (0.04 $\mu$g/ $\mu$L) was either treated with Asc and Cr(VI) (0−240 $\mu$M) at molar ratios of 0.5−2 for 2 h at 37 °C in HEPES buffer or incubated in acid buffer (10 mM sodium citrate, 10 mM sodium phosphate, 10 mM NaCl, pH 5.0) for 10 min at 70 °C as a positive control. Following treatment, samples were filter-dialyzed into 10 mM HEPES/ 100 mM potassium chloride and quantified fluorometerically. Aliquots (40−50 ng) were digested with recombinant *E. coli* endonuclease IV/*nfo* (0.5 unit) (Trevigen, Inc., Gaithersburg, MD) for 1 h. Both digested and uncut aliquots of each sample were mixed with 6× loading buffer and resolved on a 1% agarose gel for 2 h. DNA bands in gels were scanned and quantified by spot densitometry. The ratio of open/nicked plasmid to supercoiled was calculated and, assuming a random distribution of lesions, the number of abasic sites/ plasmid was determined by the Poisson distribution as described for the QPCR analysis.

*Statistical Analysis.* Analysis of variance (ANOVA) was utilized for establishing concentration-dependent effects (GraphPad Prism, GraphPad Software Inc., San Diego, CA).

## RESULTS

*Concentration-Dependent Formation of Cr−DNA Adducts and PALs.* Initial experiments were designed to determine concentration-dependent formation of Cr−DNA adducts and PALs in isolated HLF DNA (0.04 $\mu$g/$\mu$L). As shown in Figure 1A, $^{51}$Cr(VI) plus Asc, at a constant Asc:Cr(VI) molar ratio of 0.5:1, produced a concentration-dependent increase in Cr−DNA adduct formation (60 $\mu$M = 20.5 Cr atoms/1.5 kb). For comparison, we performed identical reactions using the primary DNA binding species of Cr, Cr(III). Incubation of DNA with increasing $^{51}$Cr(III) concentrations produced a similar trend in Cr−DNA binding albeit at 4−13-fold greater total adduct levels than those observed for Cr(VI)/Asc. Specifically, 60 $\mu$M Cr(III) generated 83.9 Cr adducts/1.5 kb. The adduct levels produced by 30−60 $\mu$M Cr(VI)/ Cr(III) were significantly greater ($P < 0.05$) than all other Cr concentrations tested.

Cr(VI) reduction leads to a complex array of DNA lesions, which present a physical obstruction to the in vitro replication of Cr-treated DNA. Previous work has demonstrated the utility of QPCR for studying Cr-induced PALs in isolated human DNA (*20*) and in Cr(VI)-treated yeast (T. O'Brien, unpublished results). As shown in Figure 1A (lines) and Figure 1B (gel), PALs were detectable, as an inhibition of *Taq*-mediated amplification of a 1.5 kb target sequence (p53: exons 5−8), in HLF DNA. At or above 15 $\mu$M Cr(VI), PALs increased in a similar fashion as Cr−DNA binding (60 $\mu$M = ∼1.7 PALs/1.5 kb). A concentration-dependent increase in PALs was also apparent above 7.5 $\mu$M Cr(III) and reached ∼5.1 PALs/ 1.5 kb at 60 $\mu$M. Although lower concentrations produced similar effects, 60 $\mu$M Cr(VI)/ Cr(III) was the lowest effective concentration that consistently produced a complete abrogation of amplification. Therefore, we used this concentration for all remaining PAL experiments.

*Effect of Increasing Asc:Cr(VI) Molar Ratios on Cr(VI) Reduction, Cr−DNA Binding, PAL, and ICL.* The molar ratio of Asc (and other reductants) to Cr(VI) in reactions can significantly impact both the types of Cr-species generated as well as the spectrum of genetic lesions that result from Cr(VI) reduction. We investigated the impact of different Asc to Cr(VI) molar ratios on the reductive metabolism of Cr(VI), Cr−DNA binding, and formation of PALs and ICLs in isolated DNA. The reduction of Cr(VI) (60 $\mu$M) was monitored in the presence of 0−720 $\mu$M Asc (up to a 12:1 molar ratio) for 2 h at 37 °C. Figure 2A shows that the concentration of unreacted Cr(VI) remaining following incubation decreased with increasing Asc concentration. At the Asc:Cr(VI) molar ratio of 0.5, only ∼40% of the Cr(VI) is reduced to DNA-reactive metabolites, explaining the difference in total adduct formation between Cr(VI) and Cr(III) shown in Figure 1A. Asc:Cr(VI) molar ratios of 2:1 and higher produced maximal Cr(VI) reduction.

The metabolic reduction of Cr(VI) generates DNA-reactive Cr species that interact with both DNA bases and the sugar−phosphate backbone (*25*). Although Cr(V) possesses an affinity for nucleic acids, the majority of Cr−DNA binding ultimately involves Cr(III) (*16*). We examined the effect that increasing Asc concentrations had on total Cr−DNA binding (i.e., mono and bifunctional Cr−DNA adducts) using human lung fibroblast (HLF) DNA treated with 60 $\mu$M $^{51}$Cr(VI). As shown in Figure 2B (line), Cr−DNA binding increased in parallel with increasing Asc:Cr(VI) ratios up to 2 ($P < 0.05$), which also produced ∼100% Cr(VI) reduction. However, at Asc:Cr(VI) ratios greater than 2, a general decrease ($P < 0.05$) in total Cr−DNA binding was observed, even though Cr(VI) reduction was complete.

To determine whether PAL formation was also sensitive to changes in Asc concentration, we performed QPCR analysis on Cr-treated HLF DNA. Figures 2B (bars) and 2C (gel) show that PALs were maximal beginning at an Asc:

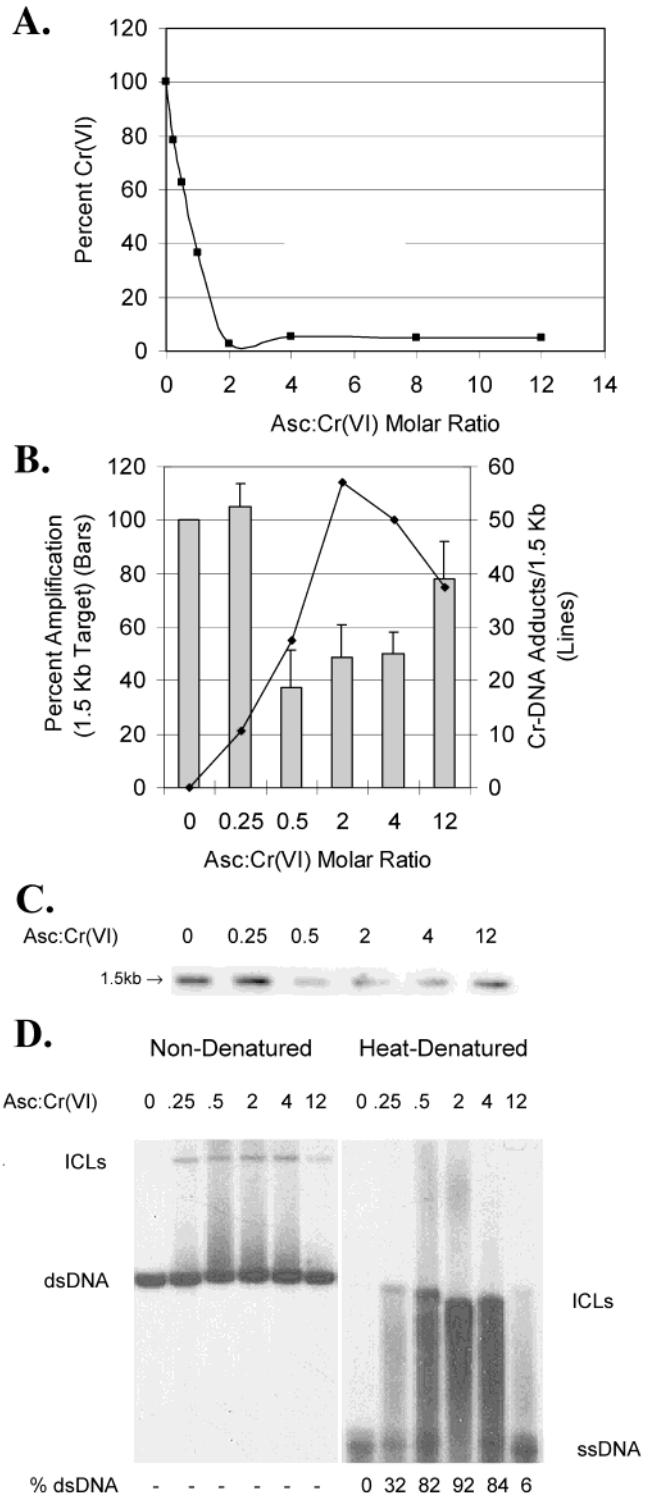


FIGURE 2: Relationship between increasing Asc:Cr(VI) molar ratios on Cr(VI) reduction (A), $^{51}$Cr−DNA binding (B), PALs (B and C), and ICLs (D). Cr(VI) (60 $\mu$M) was incubated with Asc at the indicated molar ratios for 2 h. (A) Percent Cr(VI) remaining following incubation with increasing Asc concentrations. (B) Comparison of QPCR target sequence amplification (bars) and total $^{51}$Cr binding (line) in HLF DNA. (C) Representative gel showing QPCR analysis of the target sequence in Cr(VI)/Asc-treated HLF DNA. (D) Detection of Cr-induced DNA interstrand cross-links in pSV2neoTS DNA by RAGE. One hundred nanograms of DNA was loaded per lane. PALs and ICLs were detected as described under Materials and Methods. dsDNA, double-stranded DNA; ssDNA, single-stranded DNA; ICLs, Cr−DNA interstrand cross-links. All data points are the mean and standard error of at least three independent experiments.

Cr(VI) ratio of 0.5 (~1.0 PAL/1.5 kb = 38% amplification) and gradually decreased at higher ratios (12:1 0.3 PAL/1.5 kb = ~80% amplification). The Asc:Cr(VI) ratio (2) that led to the highest levels of Cr−DNA adducts (2-fold greater than 0.5) did not produce significantly higher levels of PALs than the 0.5 ratio. Treatment of DNA with either Cr(VI) or Asc alone had no measurable effect on PAL formation (not shown). Although maximal PALs were initially observed at a ratio of 0.5:1, we obtained similar results at ratios up to 4:1.

ICLs have been hypothesized to be a primary polymerase arresting lesion formed by carcinogenic Cr(VI) in cells and DNA (*12*, *26*). To relate ICLs to Cr−DNA adduct and PAL formation, we treated pSV2neoTS DNA with 60 $\mu$M Cr(VI) at molar ratios of Asc:Cr(VI) identical to those shown in Figure 2A and B. ICLs were detected using renaturing agarose gel electrophoresis (RAGE) and Southern hybridization (*12*, *18*). As Figure 2D shows, interplasmid ICLs were clearly visible under nondenaturing conditions (left panel) as distinct bands that migrated with slower electrophoretic mobility than linear plasmid DNA (dsDNA) and were detectable at the lowest Asc:Cr(VI) ratio (0.25). Following heat denaturing (right panel), ICLs were evident as bands that still migrated as double-stranded DNA. Maximal DNA cross-linking was observed between Asc:Cr(VI) ratios of 0.5 and 4 (80−90% dsDNA). At ratios of 0.5−4 (right panel), the dsDNA exhibited an increased electrophoretic mobility which may have been due to structural/electrochemical alterations in DNA caused by extensive cross-linking under denaturing conditions. Similar to the Cr−DNA binding and PAL data, Asc:Cr(VI) ratios above 4 led to a gradual decrease in ICLs which was essentially absent at a 12:1 ratio.

*Abrogation of Cr−DNA Binding by EDTA, Mannitol, and $MgCl_2$.* To further elucidate the role of direct Cr−DNA interactions in PAL development, we performed reactions under conditions aimed at specifically inhibiting either Cr(III)− or Cr(V)−DNA binding or Cr−DNA−phosphate interactions. EDTA, a strong chelator of Cr(III) ions ($K_a$ = $10^{24}$) (*27*), disrupts Cr(III)-induced ICLs and DPCs under alkaline conditions (*28*). At an Asc:Cr(VI) ratio of 0.5, EDTA co-treatment led to a marked reduction in Cr−DNA adduct levels (Figure 3A). Specifically, adduct levels were reduced from 26.2 Cr adducts/1.5 kb in the absence of EDTA to only 3.9, 1.3, and 0.4 Cr adducts/1.5 kb following co-treatment with 0.1, 1.0, and 10 mM EDTA, respectively. Similar effects were noted at an Asc:Cr(VI) ratio of 2 (data not shown), which resulted in maximal Cr−DNA binding (Figure 2B). EDTA co-treatment with Cr(III) also effectively inhibited Cr(III)−DNA binding in a concentration-dependent manner (Figure 3A). Cr(III) alone produced 85.5 Cr adducts/1.5 kb, and 10 mM EDTA reduced Cr(III) binding to 0.3 Cr adduct/1.5 kb.

Cr(V) species have been implicated in the genotoxicity of Cr(VI), particularly at lower (<2) Asc:Cr(VI) molar ratios (*29*). Mannitol, a hydroxyl radical scavenger, has been reported to decrease both Cr−DNA binding and PAL formation in plasmid DNA (*17*). This finding was attributed to the ability of mannitol to stabilize/sequester reactive Cr(V) species following the reduction of Cr(VI) by Asc. In the present study, the simultaneous addition of mannitol with Cr(VI) [Asc:Cr(VI) ratio of 0.5] markedly inhibited Cr−DNA binding (Figure 3B) from 26.2 Cr adducts/1.5 kb in

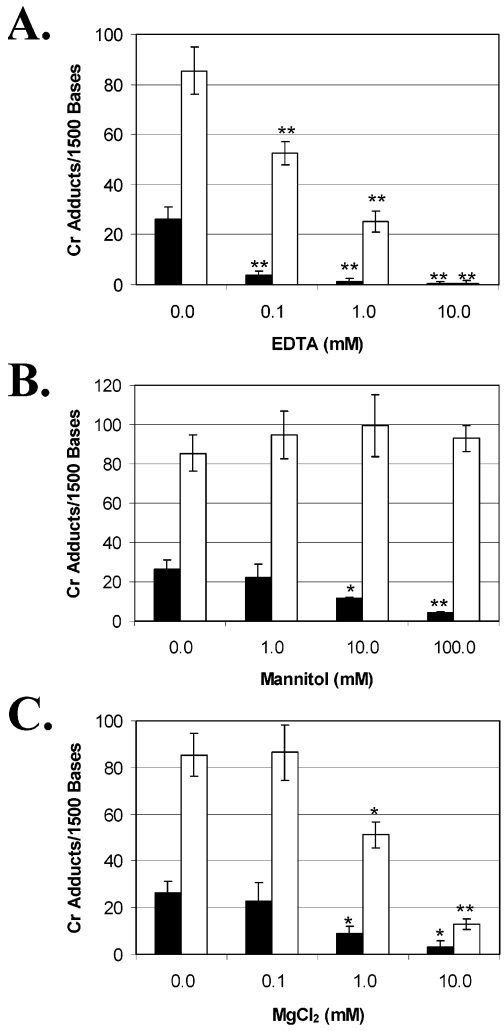


FIGURE 3: Modulation of $^{51}$Cr−DNA binding by EDTA (A), mannitol (B) co-treatment or $MgCl_2$ (C) pretreatment. DNA was treated with Cr(VI) (60 $\mu$M) and Asc (30 $\mu$M) (closed bars), or 60 $\mu$M Cr(III) (open bars), for 2 h. The data are the mean and standard error from at least three independent experiments. (* and ** indicate significantly different from controls at $P < 0.05$ and $P < 0.01$, respectively.)

the absence of mannitol, to 22.3, 11.4, and 4.1 Cr adducts/1.5 kb at 1, 10, and 100 mM mannitol, respectively. Similar mannitol-dependent effects on Cr−DNA binding were observed at higher Asc:Cr(VI) (2:1) ratios (data not shown). In contrast to Cr(VI)/Asc, Cr(III)−DNA binding was not reduced by the presence of mannitol.

Cr(III) and Cr(V) interact with DNA phosphate groups which represent a potentially important component of Cr-induced mutagenesis (*11, 30, 31*). $Mg^{2+}$ ions are known to bind specifically at DNA phosphate residues (*32*). Preincubation of DNA for 1 h with increasing concentrations of $MgCl_2$, to allow for the complete formation of $Mg^{2+}$−DNA phosphate complexes, reduced Cr−DNA binding from 26.2 to 15.2, 6.1, and 2.2 Cr adducts/1.5 kb at 0, 0.1, 1.0, and 10 mM $MgCl_2$, respectively (Figure 3C). $MgCl_2$ had similar inhibitory effects on Cr−DNA binding at Asc:Cr(VI) ratios of 2:1 (data not shown). Similarly, 60 $\mu$M Cr(III) alone (or with 0.1 mM $MgCl_2$) produced approximately 86 adducts/1.5 kb in the absence of $MgCl_2$, but only 51.2 and 13.0 Cr−DNA adducts/1.5 kb following pretreatment with 1 and 10 mM $MgCl_2$, respectively.

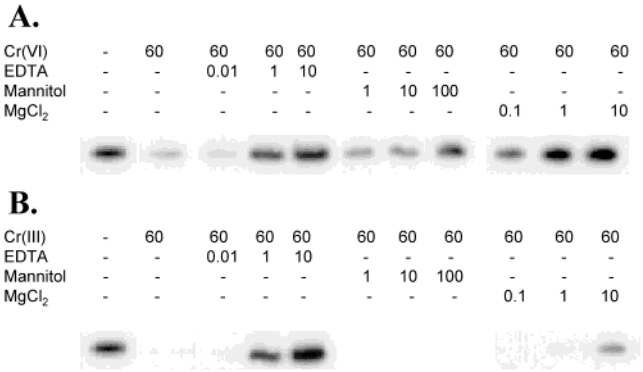


FIGURE 4: Abrogation of PALs by EDTA, mannitol co-treatment or $MgCl_2$ pretreatment. HLF DNA was treated with Cr(VI) (60 $\mu$M) plus Asc (30 $\mu$M) (A), or 60 $\mu$M Cr(III) (B), for 2 h in the presence of the indicated concentrations (mM) of EDTA or mannitol. DNA was preincubated with the indicated concentrations (mM) of $MgCl_2$ for 1 h prior to the addition of Cr(VI)/Asc or Cr(III).

*PALs Are Dependent upon Direct Metal−DNA Phosphate Interactions.* Because Cr−DNA binding was significantly altered by EDTA, mannitol, and $MgCl_2$, we determined the effect of these agents on PAL formation in HLF DNA. At 60 $\mu$M Cr(VI) [Asc:Cr(VI) ratio of 0.5], co-incubation with 0, 0.01, 1, or 10 mM EDTA reduced PAL formation in a concentration-dependent manner (Figure 4A). For Cr(III) (60 $\mu$M) (Figure 4B), inclusion of EDTA (0, 0.01, 1, 10 mM) also led to a reduction in PALs. In the absence of Cr(VI) and/or Asc, EDTA (10 mM) had no effect on the amplification of the target sequence (data not shown).

The abrogation of Cr−DNA adduct formation by mannitol (Figure 3B) implied that Cr(V) is a critical intermediate for Cr−DNA interactions following Asc reduction. Figure 4A shows that the co-addition of 1, 10, or 100 mM mannitol to reactions containing 60 $\mu$M Cr(VI) [Asc:Cr(VI) ratio of 0.5] also reduced PAL production. Consistent with the DNA binding data (Figure 3B), mannitol had no effect on PAL formation in HLF DNA from reactions containing 60 $\mu$M Cr(III) (Figure 4B), nor did it alone affect the amplification of the target sequence (data not shown).

The results of our $MgCl_2$/Cr−DNA binding experiments (Figure 3C) indicated that Cr−DNA phosphate complexes were important Cr−DNA interactions. Preincubation with $MgCl_2$ (10 mM) greatly decreased PAL development after 60 $\mu$M Cr(VI) [0.5:1 Asc:Cr(VI) ratio] or Cr(III) treatment of HLF DNA (Figure 4A and Figure 4B, respectively). Similar results were observed in reactions containing Asc and Cr(VI) at a ratio of 2 (data not shown). $MgCl_2$ did not affect the amplification of the target sequence in the absence of Cr(IV) and/or Asc (data not shown).

*Abrogation of ICLs by EDTA, Mannitol, and $MgCl_2$.* The interdependence of ICLs on Cr−DNA binding was investigated following co-treatment with EDTA, mannitol, and $MgCl_2$. Incubation of pSV2neoTS DNA with Cr(VI) (60 $\mu$M) [Asc:Cr(VI) ratio of 0.5] in the presence of EDTA or mannitol or following pretreatment of DNA with $MgCl_2$ completely blocked ICL formation (Figure 5) at concentrations that led to maximal inhibition of Cr−DNA binding and PAL development (Figures 3 and 4, respectively). Specifically, we found that the amount of plasmid DNA migrating as double-stranded was 55% in the presence of Cr(VI)/Asc,

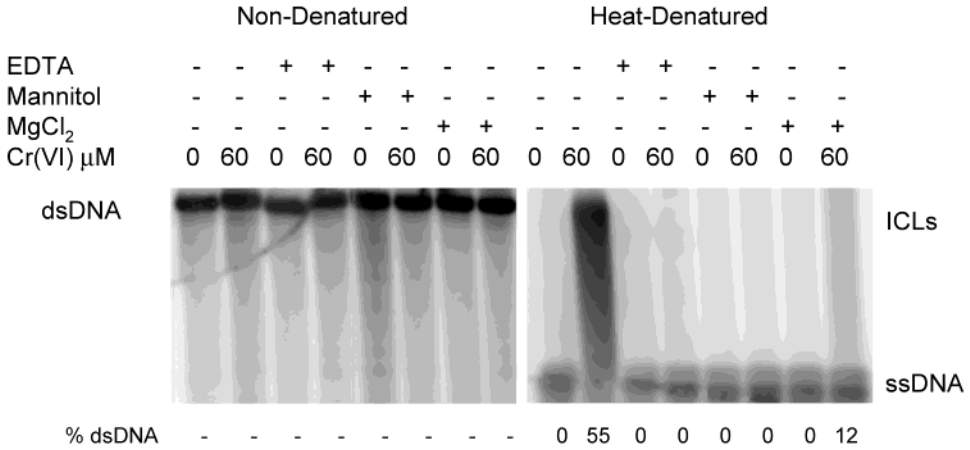


FIGURE 5: Effects of EDTA, mannitol, and $MgCl_2$ on Cr-induced ICLs. DNA was treated as described in Figures 3 and 4, and ICLs were detected by RAGE. dsDNA, double-stranded DNA; ssDNA, single-stranded DNA; ICLs, Cr−DNA interstrand cross-links.

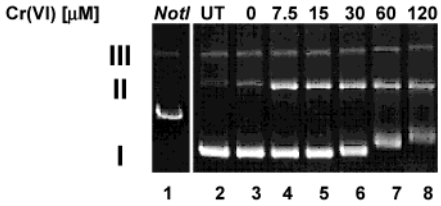


FIGURE 6: Asc-mediated reduction of Cr(VI) alters the electrophoretic mobility of plasmid DNA but does not result in DNA strand breaks. pSV2neoTS DNA (0.04 $\mu$g/$\mu$L) was incubated with 0−120 $\mu$M Cr(VI)/Asc [Asc:Cr(VI) ratio of 0.5] for 2 h (lanes 3−8). Samples (0.2−0.4 $\mu$g) were resolved electrophoretically on a 1% agarose gel. Lanes 1, 2, and 3 contain *Not*I-linearized, untreated, and vehicle control pSV2neoTS DNA, respectively. Form I: supercoiled. Form II: nicked/dimerized plasmid. Form III: concatamerized plasmid.

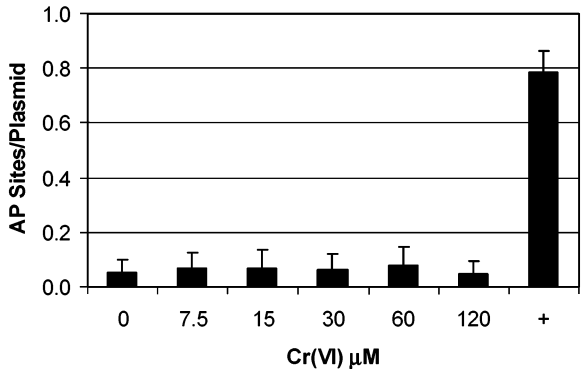


FIGURE 7: Cr(VI)/Asc does not result in the extensive formation of abasic sites. pBR322 DNA (0.04 $\mu$g/$\mu$L) was incubated with Cr(VI) and Asc [Asc:Cr(VI) ratio of 0.5], washed and digested with endonuclease IV for 1 h, and resolved on a 1% agarose gel for 2 h. Acid/heat (70 °C)-mediated depurination (+) was used as a positive control in all gels. Data are the mean and standard error from two independent experiments.

was completely absent after EDTA or mannitol co-treatment, and was 12% after $MgCl_2$ pretreatment.

*The Reduction of Cr(VI) by Asc Does Not Lead to DNA Strand Breaks.* Cr(VI) reduction can potentially produce a variety of intermediate oxygen and carbon-based radical species that are capable of producing DNA strand breaks (*8*, *14*). Such lesions could reduce the amount of amplifiable template DNA leading to polymerase arrest in in vitro replication assays. To evaluate the formation of DNA strand breaks in our study, we monitored the relaxation of supercoiled plasmid DNA following Cr(VI) treatment [Asc:Cr(VI) ratio of 0.5]. As seen in Figure 6, increasing Cr(VI) concentrations impeded the mobility of supercoiled (form I) pSV2neoTS DNA which has previously been attributed to Cr−DNA binding (*33*). However, no concomitant decrease in the intensity of form II (nicked/dimerized) or linearized plasmid was observed, indicating that neither single- nor double-strand breaks were produced during the reaction, respectively. Even conditions [Asc:Cr(VI) molar ratio of 2] that led to complete Cr(VI) reduction and maximal Cr−DNA binding failed to reveal detectable DNA strand breaks (data not shown). Because EDTA, mannitol, and $MgCl_2$ all produced similar decreases in Cr−DNA adduct levels and PAL, we also examined the mobility of pSV2neoTS treated with Cr(VI)/Asc. All three treatments reversed the retardation of supercoiled plasmid DNA resulting from Cr(VI) treatment (data not shown).

*The Reduction of Cr(VI) by Asc Does Not Result in the Formation of Abasic Sites.* In vitro data suggested that Cr(VI) reduction may lead to the generation of abasic sites in DNA (*34*−*36*). Because a significant number of abasic sites could theoretically impair the amplification of the target sequence in the QPCR assay, we measured the incision of abasic sites in Cr(VI)/Asc-treated [Asc:Cr(VI) ratio of 0.5] pBR322 DNA by the *E. coli* AP endonuclease IV (*nfo*). As can be seen in Figure 7, Cr(VI) did not produce any significant increases in endonuclease IV-sensitive abasic lesions (∼0.1 abasic site/plasmid) even at high concentrations (120 $\mu$M and data not shown). Reactions performed in the presence of a 2-fold molar excess of Asc also failed to produce abasic sites (data not shown). In contrast, DNA incubated in acid buffer at 70 °C led to a marked increase in abasic sites (∼0.8 abasic site/plasmid).

## DISCUSSION

The in vitro base-specific arrest of DNA polymerases on Cr-treated plasmid DNA has been well-documented (*12*, *18*, *19*). Although Cr(VI) reduction produces several types of DNA lesions, neither Cr−monadducts nor Cr−DPC (GSH) interfere with polymerase progression (*20*). One lesion produced directly by Cr, a DNA−Cr−DNA interstrand cross-link (ICL), has been associated with the base-specific

obstruction of DNA polymerase replicative activity (*12*, *18*). Other lesions (oxidized bases, DNA strand breaks, AP sites) produced by Cr(VI) reduction could also result in the arrest of DNA polymerases in in vitro replication assays (*15*, *21*, *22*). However, little information is available that describes the relative contribution of these lesions to Cr-induced polymerase arrest. The aim of this investigation was to determine the role of Cr−DNA binding and ICLs in the development of PALs. Our data strongly suggest that PALs primarily result from ICLs, and not DNA strand breaks or AP sites. Furthermore, the data indicate that phosphate moieties may play an important role in Cr−DNA interactions including ICL formation.

An apparent association was observed between Cr−DNA binding and the development of PALs in this study. QPCR analysis indicated that 60 $\mu$M Cr(VI) generated approximately 1−2 PALs per 1.5 kb. At this concentration, we also detected 20−30 Cr−DNA adducts per 1.5 kb. Based on these data, we estimate that less than 10% of Cr−DNA adducts participate in the development of polymerase arrest. Moreover, the data in Figures 2 and 5 strongly indicate that ICLs are the primary lesion responsible for Cr-induced polymerase arrest in reactions carried out in HEPES buffer and using Asc as the reductant. ICLs have been detected in human cells treated with Cr(VI) (*26*), and we have recently shown that both human cells (*37*) and yeast (T. O'Brien, unpublished data) deficient in ICL repair are hypersensitive to Cr(VI). Collectively, these data suggest that ICLs may play an important role in Cr-toxicity and possibly mutagenesis. However, more detailed, quantitative in vivo analysis is required to conclusively identify ICLs as the primary lethal lesion formed by Cr in cells.

The relative amount of high-valent Cr intermediates [Cr(IV)/Cr(V)], carbon-based and ascorbyl radicals produced during the reduction of Cr(VI) by Asc is highly dependent upon the relative ratios of reactants and buffer composition (*29*, *38*). In HEPES buffer, the production of Cr(V) and carbon-based radicals derived from Asc linearly increases with Asc:Cr(VI) ratios up to 1, but rapidly decreases above this level which, instead, favors the two-electron reduction of Cr(VI) directly to Cr(IV) (*29*). In addition, the production of PALs and ICLs is sensitive to the ratio of Asc to Cr(VI) (Figure 2) (*12*). Although we did not observe the complete abrogation of Cr−DNA binding as Stearns et al. reported (*29*), our data are still consistent with that investigation in that increasing the molar ratio of Asc to Cr(VI) beyond 2 led to a general reduction in Cr−DNA adducts (Figure 2B). It is likely that, at these higher relative levels of Asc, more coordinate sites on Cr are occupied by Asc and, thus, prevent further Cr−DNA interaction. Recent work has estimated that the formation of Asc−Cr−DNA cross-links accounts for approximately 25 and 6% of the total Cr−DNA adducts in in vitro treated DNA and DNA isolated from A549 lung carcinoma cells, respectively (*39*). Our study found that at Asc:Cr(VI) ratios of 12, fewer PALs were observed compared to a ratio of 0.5 (Figure 2). The Cr−DNA binding data and the fact that PAL and ICL formation was reduced at increasing molar ratios of Asc:Cr(VI) suggest that higher relative concentrations of Asc interfere with the formation of both mono- and bifunctional Cr−DNA adducts. We have reported similar results with higher concentrations of glutathione, which inhibited both PALs and ICLs, independent of alterations in Cr−DNA binding (*20*).

The interaction of $Mg^{2+}$ with negatively charged DNA phosphate groups is important in the stabilization of DNA structure (*32*). Similarly, the affinity of electropositive chromium for DNA phosphates has also been described which may involve chelation of Cr by the oxygen atom of phosphate (*9*, *16*, *30*). Indeed, an abrogation of Cr−DNA binding has been observed in reactions containing phosphate buffer (*33*) or in DNA pretreated with $MgCl_2$, suggesting that Cr(III)−DNA phosphate interactions may be an important aspect of Cr genotoxicity (*31*, *39*). In the present study, it is intriguing that $MgCl_2$ pretreatment greatly reduced Cr−DNA binding and PAL formation (Figures 3 and 4, respectively). Interestingly, a small amount of cross-linked dsDNA (12%) remained following $MgCl_2$ pretreatment (Figure 5), which may constitute ICLs exclusively involving DNA bases. Previous work has implicated the Cr-induced PALs as guanine-specific lesions (*12*). Thus, we are intrigued that the present study provides evidence that Cr−DNA phosphate interactions play a surprisingly instrumental role in the bifunctional adduction of Cr to DNA. Perhaps one explanation may be related to recent work that has provided several possible structures for phosphate-based Cr−DNA monoadducts (*33*) and evidence for an N-7 guanine−Cr−phosphate chelate (*11*). The existence of such a novel lesion supports the idea that an ICL involving both DNA phosphate and base moieties is plausible. Detailed structural analysis of Cr−DNA interactions is required to further elucidate the exact nature of bifunctional Cr−DNA adducts involving DNA phosphate.

In vitro replication assays (primer extension, PCR) are highly sensitive means for identifying lesions that prevent polymerase progression on template DNA. While we hypothesize that ICLs are the primary PAL formed by Cr, other lesions could potentially produce similar results. DNA strand breaks in either one or both strands could significantly impede replication of template DNA. Although Cr(VI) reduction generates strand breaks, we failed to observe these lesions using the common supercoiled plasmid relaxation assay. Even at a 2:1 Asc to Cr(VI) ratio, which produced maximal Cr−DNA binding (Figure 2B), no strand breaks were detected (data not shown). Although bypass DNA polymerases can insert bases opposite AP sites in template DNA (*40*), these lesions have been reported to cause *Taq* polymerase stoppage (*21*, *22*). Several studies have reported the production of abasic sites in Cr-treated DNA (*13*, *36*). However, we were unable to detect any concentration-dependent increases in AP sites that were sensitive to endonuclease IV (a class II AP endonuclease) digestion, indicating that these lesions are not significantly formed by the Asc-mediated reduction of Cr(VI). Our results are similar to those previously reported for the reduction of Cr(VI) with Cys, which also failed to result in abasic site generation (*38*).

Cells do not exhibit any active efflux mechanisms for the removal of Cr(III) and, therefore, can accumulate the metal (*41*) to intracellular concentrations as high as 1 mM following treatment with genotoxic levels of Cr(VI) (*6*). Moreover, intranuclear concentrations of Cr have been shown to be significantly greater than the extracellular medium (*42*). Although the intracellular levels of Asc can vary, attainment of millimolar concentrations has been reported (*43*−*45*). Based on the data from this and other studies, we have

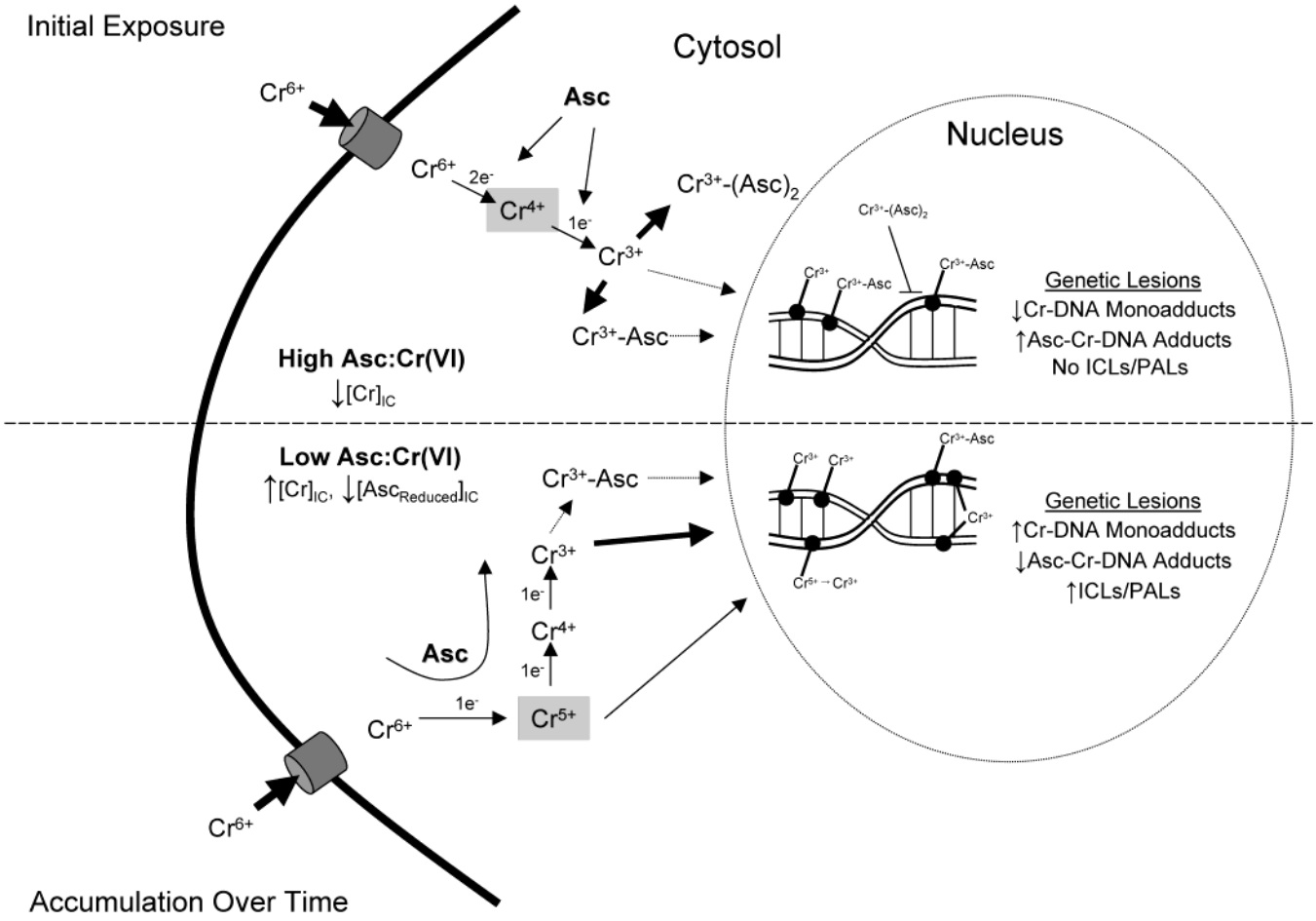


FIGURE 8: Proposed model of Cr−DNA interactions following Asc reduction within a Cr(VI)-treated cell. Hypothetical relative contribution of each Cr species to DNA damage is portrayed by arrow thickness. The dotted arrow implies a relatively minor contribution. The known contribution of other intracellular reductants is discussed in the text, but not portrayed. Note that all metabolic pathways are drawn in the cytosol for clarity ($Cr^{3+}$ = Cr−DNA monoadducts; $Cr^{3+}$−Asc = Asc−Cr−DNA adducts; $Cr^{3+}$−$(Asc)_2$ = Cr−Asc complexes).

proposed a model that describes the dynamic interrelationships that exist between various Cr−DNA lesions and different Asc:Cr(VI) molar ratios within naive cells treated with Cr(VI) (Figure 8, upper panel). In this model, immediately following exposure to a relatively noncytotoxic concentration of Cr(VI), the intracellular Asc:Cr(VI) molar ratio would be extremely high with the majority of chromate residing in the extracellular milieu and entering the cell through nonspecific anionic transporters (*4, 46*). At these ratios (>4:1), the kinetically favored reduction of Cr(VI) by an excess of Asc would follow an initial two-electron pathway leading to the formation of a transient Cr(IV) species and ultimately Cr(III) (*29, 39*). These initially high Asc:Cr(VI) ratios would result in the extensive formation of both Cr(III)−$(Asc)_2$ complexes, which display a low affinity for DNA, and a significant amount of Asc−Cr−DNA complex/ternary adducts (*39*). A general decrease in absolute Cr−DNA binding would be observed with lower levels of binary Cr−DNA monoadducts and an almost complete abrogation of ICL and PAL formation (*29, 39*). We propose that, in addition to Cr(III)−$(Asc)_2$ complexes, the preferential formation of Asc−Cr−DNA ternary adducts is a primary factor responsible for the prevention of Cr-induced ICLs (PALs) by inhibiting the interaction between Cr(III) and the base (guanine)/phosphate of the complementary DNA strand. Therefore, Asc [at high Asc:Cr(VI) ratios] would initially provide a cyto-protective role based on sequestration of reactive Cr(III) and prevention of potentially toxic ICLs (PALs). However, the abrogation of ICL formation would be at the expense of producing Asc−Cr−DNA cross-links which may exhibit increased mutagenic potential (*39*).

As more Cr accumulates within the cell, and reduced Asc is depleted, a gradual shift toward a lower Asc:Cr ratio would be expected (Figure 8, lower panel). Consequently, the spectrum of Cr-associated DNA damage will favor the development of both mono- and bifunctional Cr−DNA adducts (ICLs) and ternary Asc−Cr−DNA monoadducts as observed at ratios of 0.5−4 in this and other in vitro studies (*29, 39*). Potentially mutagenic, but not polymerase arresting, Asc−Cr(III)−DNA ternary adducts would also be produced at these lower Asc:Cr(IV) ratios, but would not represent the predominant DNA base modification (*39*). Lower relative Asc:Cr(VI) ratios would also favor a one-electron reduction mechanism which would result in the formation of DNA-reactive Cr(V) intermediates (*7, 29*) (Figure 8, lower panel). Not shown in Figure 8, as intracellular reduced Asc levels are lowered, a transition toward a thiol-mediated (GSH, cysteine) reductive pathway would be anticipated. Such a mechanism would lead to the extensive formation of protein−Cr(III)−DNA cross-links which preclude ICL/PAL development (*20*), but are mutagenic (*31, 33*). Therefore,

the relative impact that multiple reductants (Asc, GSH, Cys) may have on this process is likely to be significant, but not known at this time.

Although a complex array of genetic lesions is produced as a consequence of Cr(VI) reduction, the direct interaction of Cr with DNA is critical for the formation of lesions capable of obstructing DNA polymerase progression. The work presented here strongly supports the importance of ICLs as the major Cr-induced PALs in treated DNA. In addition, this study is the first to provide evidence for a role of coordinate Cr−DNA phosphate interactions in the formation of Cr-induced ICLs (PALs).

## REFERENCES


1. IARC (1990) *Monograph on the Evaluation of Carcinogenic Risk to Humans. Chromium, Nickel and Welding*, Vol. 49, IARC, Lyon, France.
2. Singh, J., Carlisle, D. L., Pritchard, D. E., and Patierno, S. R. (1998) *Oncol. Rep. 5*, 1307−1318.
3. De Flora, S. (2000) *Carcinogenesis 21*, 533−541.
4. Arslan, P., Beltrame, M., and Tomasi, A. (1987) *Biochim. Biophys. Acta 931*, 10−15.
5. Buttner, B., and Beyersmann, D. (1985) *Xenobiotica 15*, 735−741.
6. Wise, J. P., Orenstein, J. M., and Patierno, S. R. (1993) *Carcinogenesis 14*, 429−434.
7. Stearns, D. M., and Wetterhahn, K. E. (1994) *Chem. Res. Toxicol. 7*, 219−230.
8. Stearns, D. M., Courtney, K. D., Giangrande, P. H., Phieffer, L. S., and Wetterhahn, K. E. (1994) *Environ. Health Perspect. 102 (Suppl. 3)*, 21−25.
9. Tsapakos, M. J., and Wetterhahn, K. E. (1983) *Chem.-Biol. Interact. 46*, 265−277.
10. Aiyar, J., Berkovits, H. J., Floyd, R. A., and Wetterhahn, K. E. (1991) *Environ. Health Perspect. 92*, 53−62.
11. Arakawa, H., Ahmad, R., Naoui, M., and Tajmir-Riahi, H. A. (2000) *J. Biol. Chem. 275*, 10150−10153.
12. Bridgewater, L. C., Manning, F. C., and Patierno, S. R. (1994) *Carcinogenesis 15*, 2421−2427.
13. Casadevall, M., da Cruz Fresco, P., and Kortenkamp, A. (1999) *Chem.-Biol. Interact. 123*, 117−132.
14. Stearns, D. M., and Wetterhahn, K. E. (1997) *Chem. Res. Toxicol. 10*, 271−278.
15. Sugden, K. D., Campo, C. K., and Martin, B. D. (2001) *Chem. Res. Toxicol. 14*, 1315−1322.
16. Zhitkovich, A., Voitkun, V., and Costa, M. (1996) *Biochemistry 35*, 7275−7282.
17. Tsou, T. C., Lai, H. J., and Yang, J. L. (1999) *Chem. Res. Toxicol. 12*, 1002−1009.
18. Bridgewater, L. C., Manning, F. C., Woo, E. S., and Patierno, S. R. (1994) *Mol. Carcinog. 9*, 122−133.
19. Bridgewater, L. C., Manning, F. C., and Patierno, S. R. (1998) *Mol. Carcinog. 23*, 201−206.
20. O'Brien, T., Xu, J., and Patierno, S. R. (2001) *Mol. Cell. Biochem. 222*, 173−182.
21. Barnes, W. M. (1994) *Proc. Natl. Acad. Sci. U.S.A. 91*, 2216−2220.
22. Fromenty, B., Demeilliers, C., Mansouri, A., and Pessayre, D. (2000) *Nucleic Acids Res. 28*, E50.
23. Manning, F. C., Xu, J., and Patierno, S. R. (1992) *Mol. Carcinog. 6*, 270−279.
24. Borges, K. M., Boswell, J. S., Liebross, R. H., and Wetterhahn, K. E. (1991) *Carcinogenesis 12*, 551−561.
25. Tamino, G., Peretta, L., and Levis, A. G. (1981) *Chem.-Biol. Interact. 37*, 309−319.
26. Xu, J., Bubley, G. J., Detrick, B., Blankenship, L. J., and Patierno, S. R. (1996) *Carcinogenesis 17*, 1511−1517.
27. Earley, J. E., and Cannon, R. D. (1965) *Aqueous chemistry of chromium(III)*, Vol. 1, Marcel Dekker, New York.
28. Singh, J., Bridgewater, L. C., and Patierno, S. R. (1998) *Toxicol. Sci. 45*, 72−76.
29. Stearns, D. M., Kennedy, L. J., Courtney, K. D., Giangrande, P. H., Phieffer, L. S., and Wetterhahn, K. E. (1995) *Biochemistry 34*, 910−919.
30. Sugden, K. D., and Wetterhahn, K. E. (1996) *Inorg. Chem. 35*, 3727−3728.
31. Voitkun, V., Zhitkovich, A., and Costa, M. (1998) *Nucleic Acids Res. 26*, 2024−2030.
32. Sander, C., and Ts'o, P. O. (1971) *J. Mol. Biol. 55*, 1−21.
33. Zhitkovich, A., Song, Y., Quievryn, G., and Voitkun, V. (2001) *Biochemistry 40*, 549−560.
34. Kortenkamp, A., Casadevall, M., and Da Cruz Fresco, P. (1996) *Ann. Clin. Lab. Sci. 26*, 160−175.
35. Casadevall, M., and Kortenkamp, A. (1995) *Carcinogenesis 16*, 805−809.
36. da Cruz Fresco, P., Shacker, F., and Kortenkamp, A. (1995) *Chem. Res. Toxicol. 8*, 884−890.
37. Vilcheck, S., O'Brien, T., Pritchard, D., Ha, L., Ceryak, S., Fornsaglio, J., and Patierno, S. (2002) *Environ. Health Perspect. Suppl.* (in press).
38. Zhitkovich, A., Shrager, S., and Messer, J. (2000) *Chem. Res. Toxicol. 13*, 1114−1124.
39. Quievryn, G., Messer, J., and Zhitkovich, A. (2002) *Biochemistry 41*, 3156−3167.
40. Haracska, L., Unk, I., Johnson, R. E., Johansson, E., Burgers, P. M., Prakash, S., and Prakash, L. (2001) *Genes Dev. 15*, 945−954.
41. Ermolli, M., Menne, C., Pozzi, G., Serra, M. A., and Clerici, L. A. (2001) *Toxicology 159*, 23−31.
42. Sehlmeyer, U., Hechtenberg, S., Klyszcz, H., and Beyersmann, D. (1990) *Arch. Toxicol. 64*, 506−508.
43. VanDuijn, M. M., Tijssen, K., VanSteveninck, J., Van Den Broek, P. J., and Van Der Zee, J. (2000) *J. Biol. Chem. 275*, 27720−27725.
44. May, J. M., Qu, Z., and Morrow, J. D. (2001) *Biochim. Biophys. Acta 1528*, 159−166.
45. Meister, A. (1994) *J. Biol. Chem. 269*, 9397−9400.
46. De Flora, S., and Wetterhahn, K. E. (1989) *Life Chem. Rep. 7*, 169−244.


BI020452J